Institute of Paper Science and Technology
Atlanta, Georgia

IPST Technical Paper Series Number 835

The Effect of Fibre Type on Bubble Size

A.E. Garner and T.J. Heindel

January 2000

Submitted to
Journal of Pulp and Paper Science

Copyright© 2000 by the Institute of Paper Science and Technology

For Members Only

INSTITUTE OF PAPER SCIENCE AND TECHNOLOGY
PURPOSE AND MISSIONS

The Institute of Paper Science and Technology is an independent graduate school, research organization, and information center for science and technology mainly concerned with manufacture and uses of pulp, paper, paperboard, and other forest products and byproducts. Established in 1929 as the Institute of Paper Chemistry, the Institute provides research and information services to the wood, fiber, and allied industries in a unique partnership between education and business. The Institute is supported by 52 North American companies. The purpose of the Institute is fulfilled through four missions, which are:

- to provide multidisciplinary graduate education to students who advance the science and technology of the industry and who rise into leadership positions within the industry;
- to conduct and foster research that creates knowledge to satisfy the technological needs of the industry;
- to provide the information, expertise, and interactive learning that enables customers to improve job knowledge and business performance;
- to aggressively seek out technological opportunities and facilitate the transfer and implementation of those technologies in collaboration with industry partners.

ACCREDITATION

The Institute of Paper Science and Technology is accredited by the Commission on Colleges of the Southern Association of Colleges and Schools to award the Master of Science and Doctor of Philosophy degrees.

NOTICE AND DISCLAIMER

The Institute of Paper Science and Technology (IPST) has provided a high standard of professional service and has put forth its best efforts within the time and funds available for this project. The information and conclusions are advisory and are intended only for internal use by any company who may receive this report. Each company must decide for itself the best approach to solving any problems it may have and how, or whether, this reported information should be considered in its approach.

IPST does not recommend particular products, procedures, materials, or service. These are included only in the interest of completeness within a laboratory context and budgetary constraint. Actual products, materials, and services used may differ and are peculiar to the operations of each company.

In no event shall IPST or its employees and agents have any obligation or liability for damages including, but not limited to, consequential damages arising out of or in connection with any company's use of or inability to use the reported information. IPST provides no warranty or guaranty of results.

The Institute of Paper Science and Technology assures equal opportunity to all qualified persons without regard to race, color, religion, sex, national origin, age, disability, marital status, or Vietnam era veterans status in the admission to, participation in, treatment of, or employment in the programs and activities which the Institute operates.

THE EFFECT OF FIBRE TYPE ON BUBBLE SIZE

Adele E. Garner and Theodore J. Heindel†
Institute of Paper Science and Technology
500 10th Street NW
Atlanta, GA 30318-5794

ABSTRACT

Flash x-ray radiography is used for gas flow visualization and bubble size measurements in three different pulp slurries. Suspensions of 1% old newspaper (ONP), copy paper (CP), and northern bleached softwood kraft (NBSK) comprise the various furnishes. For a fixed gas flow rate, the flow conditions are churn-turbulent in the fibre suspensions while bubbly flow is observed in an air/water reference condition. Bubble size measurements are obtained in the various systems, and bubbles are classified as either small ($d \leq 12$ mm) or large ($d > 12$ mm). The number of small bubbles decreases and the number of large bubbles increases as the cellulose fibre length increases. All small bubbles follow similar distributions and are characterized by a single lognormal bubble size distribution.

KEYWORDS

Bubble size distribution; Fibre suspension; Flotation deinking; Flow visualization

---

† Corresponding author, e-mail: ted.heindel@ipst.edu

INTRODUCTION

Flotation deinking is a unit operation used to remove contaminants (primarily inks and toners) from recovered paper, and is employed when ever ink-free recovered paper is desired, such as in processing old newspaper (ONP) or mixed office waste (MOW). Bubble size can have a significant effect on the flotation deinking performance [1, 2], but recording bubble size in a fibre suspension can be difficult [2, 3]. Recently, flash x-ray radiography (FXR) has been used to record bubble size in fibre suspensions at consistencies as high as 1.5% [4, 5].

Heindel and Garner [5] determined that the presence of fibre in a suspension promoted large bubble formation and lead to churn-turbulent flow conditions. This flow pattern is characterized by large bubbles creating violent oscillations in the fluid motion [6]. Small bubbles were still present in the fibre suspension, but the number of large bubbles increased with increasing fibre consistency. It was further shown that the small bubble size distribution, defined as bubbles with an equivalent diameter $d \leq 12$ mm, was independent of fibre consistency [5].

This study extends the work of Heindel and Garner [5] and investigates the effect of fibre type on bubble size. Both mechanical and chemical pulps are considered while the consistency is fixed at 1% by mass, common in flotation deinking operations.

EXPERIMENTAL PROCEDURES

A schematic representation of the experimental setup is shown in Fig. 1. The bubble column was identical to that used by Heindel and Garner [5] and can be likened to a 1 m tall graduated cylinder with a rectangular cross-section of 20 cm × 2 cm. Compressed and filtered air was injected into the base of the column through a sintered bronze sparger with a nominal pore

diameter of 40 μm. This was attached to the end of a flexible air line and placed on the bottom of the column. The air line was positioned near the column wall such that it did not interrupt the bulk bubble flow patterns. A volumetric air flow rate of 2 liters per minute was fixed for all experiments. This corresponded to a constant superficial gas velocity, defined as the volumetric gas flow rate divided by the column cross-sectional area, of 0.83 cm/s. The bubble column was charged by filling it from the top with 3.2 L of the desired fibre slurry, corresponding to a column fluid height of 80 cm. This allowed for fluid expansion in the bubble column during air injection.

The systems of interest were composed of deionized water with or without cellulose fibre at 1% consistency. Three different fibre types were used: (1) old newspaper (ONP), (2) standard copy paper (CP), and (3) northern bleached softwood kraft dry lap pulp (NBSK). All fibre samples were unprinted and free of ink and dirt. The various fibre types were reslushed following TAPPI Method T 205 om-88 [7]; however, deionized water was used, and disintegration was performed at 1.2-1.3% consistency. The 1% fibre suspensions were prepared by diluting the reslushed stock with deionized water. Representative fibre samples were analyzed to determine a weight-weighted average fibre length (Kajaani FS-100 fibre length analyzer) and ash content (TAPPI Method T413 om-93 [8]). Additionally, a filtrate sample from each suspension was obtained to determine the liquid surface tension. These results are summarized in Table 1. A reference condition of an air/water system (no fibre) is also provided.

The x-ray unit was a 300 keV HP 43733A flash x-ray system (currently supported by Maxwell Physics International, San Leandro, CA, USA), which generated a 30 nanosecond x-ray pulse. The x-ray tube schematically shown adjacent to the bubble column in Fig. 1 was actually

located perpendicular to the column face. The fast x-ray pulse provided stop-motion x-rays of gas bubbles rising through the fibre suspension. Complete details of the FXR procedures have been outlined by Heindel and Monefeldt [9]. A single 20 cm × 25.2 cm x-ray negative was exposed during each discharge of the x-ray unit.

Image analysis using Optimas image analysis software was performed on the developed x-ray negatives. The pixel size for this analysis was 0.14 mm/pixel and bubbles larger than 1 mm in diameter were analyzed. Bubble size distributions were obtained from multiple x-ray images encompassing a column height of approximately 25-45 cm from the column base. Bubble areas were recorded and converted to equivalent bubble diameters, defined as the diameter of the circle whose area was equal to that of the bubble image.

RESULTS

Figure 2 shows representative FXR images taken in the experimental facility encompassing a column height of approximately 25-45 cm from the column base. The volumetric gas flow rate in all images is constant at 2 L/min. The dark regions represent air bubbles, and the air line is apparent on the left-hand side of each radiograph. These digitized images provide a qualitative picture of the gas flow patterns within the various fibre suspensions. Detailed descriptions of the overall gas flow patterns within the entire bubble column for the air/water and NBSK systems have been provided by Heindel and Garner [5].

The air/water system (Fig. 2a) provides a fibre-free reference. In this case, the majority of the bubbles are uniform in size and well dispersed throughout the column. The general upward gas flow is characterized by an oscillating serpentine pattern encompassing the entire column.

Backmixing (regions of fluid recirculation) entrains some of the bubbles, but they eventually rise with the bulk gas flow. The gas flow regime for this condition is generally termed bubbly [6]. This gas flow regime would be beneficial for any process requiring a maximum gas/liquid interfacial area.

When 1% ONP fibre is added to the system, many small bubbles are still present, but large bubbles are also observed (Fig. 2b). Large bubbles are defined following the criteria of Clift et al. [10] which specifies when wall effects influence the bubble shape. For this geometry, when the equivalent bubble diameter is $d > 12$ mm, bubbles are identified as large and are influenced by the column walls. In contrast, when $d \leq 12$ mm, the bubbles are termed small and are assumed to be uninfluenced by the column walls. Others have also differentiated between large and small bubbles found in bubble columns [11-14]. For example, De Swart et al. [13] defined any bubble larger than 10 mm in diameter as large. One unique property of these large bubbles is that they undergo frequent coalescence and breakup [12, 13].

The large bubbles in Fig. 2b rise in a serpentine fashion, but do not travel over the entire column width. The serpentine movement also creates fluid recirculation cells and backmixes some of the small bubbles. These bubbles eventually become entrained in the upward bulk flow. The flow conditions observed here would be considered churn-turbulent, where the large bubbles create violent oscillations in the fluid motion [6]. As previously shown [5, 9, 15], the presence of fibres promote the transition from bubbly to churn-turbulent flow.

Figure 2c shows a representative FXR image for the 1% CP system. A very large spherical-capped bubble is captured in the center of the image. Small bubbles are also observed but are fewer in number than in the ONP system. Churn-turbulent flow conditions also prevail

for this condition. Similar results are obtained for 1% NBSK (Fig. 2d). However, the number of small bubbles has further decreased.

Churn-turbulent flow conditions are observed in all three fibre systems while bubbly flow is recorded in the air/water system for the same volumetric air flow rate. Large and small bubbles are also observed for the various fibre types. The major difference between the fibre types is in the bubble population where the total number of bubbles per image decreases and the percentage of large bubbles increases as fibre length increases. This is shown in Table 2. Longer cellulose fibres clearly decrease the bubble population for a fixed air injection rate. This is caused by the increase in large bubble formation due to bubble coalescence.

Also presented in Table 2 is the average bubble size for each experimental condition, which was obtained from multiple FXR images. It appears that the average bubble size is similar for the air/water and ONP conditions, and similar for the CP and NBSK conditions. However, these average values have large standard deviations associated with them, particularly for the various fibre data, because of the few number of large bubbles ($d > 12$ mm) present in each population.

The cumulative number density of the bubble size population is shown in Fig. 3. Over 92% of all bubbles are smaller than 6 mm in equivalent diameter, and there are very few bubbles in the 6-12 mm size range. The right-most data points in Fig. 3 represent all bubbles with $d > 12$ mm, and account for the remaining bubbles in the total population. As shown in Table 2 and Fig. 3, the number of these large bubbles increases with increasing fiber length.

The bubble size distribution for each fibre type follows a similar shape. The ONP fibre has more smaller bubbles than the other systems, including water. This may be due to carry-over

of various surface active agents in the ONP furnish, as well as from the ONP processing steps. The filtrate from this furnish has the lowest surface tension (Table 1) which would produce smaller stable bubbles [10]. However, the filtrate from the NBSK furnish also has a relatively low surface tension, but the bubble size distribution in this furnish follows the water data until approximately the 70th percentile. Therefore, it is hypothesized that additional constituents from the ONP system chemistry also affect bubble formation and size and are responsible for the smaller bubble sizes. Large bubbles (d > 12 mm) are also found in the ONP furnish and account for 1.2% of the total bubble population. The large bubble class is not recorded in the air/water reference system, but is observed in all fibre systems.

Following Heindel and Garner [5], the similarity in the bubble size distributions may be described by known distribution functions, but neither normal, lognormal, nor gamma distributions describe the total bubble population. However, the small bubble population (d ≤ 12 mm) in each furnish can be described by a lognormal distribution of the form

$$Cum_{LN} = \int_0^x \frac{1}{y\sigma_{LN}\sqrt{2\pi}} \exp\left[-\frac{1}{2}\left(\frac{\ln(y)-\mu_{LN}}{\sigma_{LN}}\right)^2\right] dy \qquad (1)$$

where y is a dummy variable, x is the parameter of interest (i.e., the bubble diameter), and μ_{LN} and σ_{LN} are the mean and standard deviation of the natural logarithm of the bubble diameters. These values are not equivalent to the mean and standard deviation of the bubble population (μ and σ, respectively), but can be related to them by [16]

$$\mu_{LN} = \ln(\mu) - \frac{1}{2}\sigma_{LN}^2 \qquad (2)$$

$$\sigma_{LN}^2 = \ln\left[1+\left(\frac{\sigma}{\mu}\right)^2\right] \tag{3}$$

All of the small bubble size data ($d \leq 12$ mm) is shown in Fig. 4 and the lognormal distribution identified by Heindel and Garner [5] is also included in this figure. The parameters in this distribution are $\mu_{LM} = 1.0$ and $\sigma_{LM} = 0.45$. Although this distribution was developed for NBSK at consistencies as high as 1.5%, it does a good job of describing the 1% CP data. Additionally, the size of the smaller bubbles in the ONP furnish is slightly over predicted by this correlation, but the distribution given by Heindel and Garner [5] provides a good bubble size *estimate*. Therefore, the lognormal bubble size distribution developed for small bubbles in a NBSK system provides an adequate estimate of the small bubble size distribution in the three furnishes considered here.

CONCLUSIONS

Bubble flow visualization and bubble size measurements were obtained for three different fibre types at a fixed fibre consistency and air flow rate. The bubble flow regime was churn-turbulent for all three furnishes, and the number of large bubbles ($d > 12$ mm) increased with increasing fibre length, while the number of small bubbles ($d \leq 12$ mm) decreased with increasing fiber length. A good approximation of the small bubble size distribution in all three furnishes was obtained by using the lognormal distribution proposed by Heindel and Garner [5], which was obtained for NBSK pulps at consistencies as high as 1.5%. Therefore, the small bubble size distribution has been shown to be independent of fibre type for the conditions of this study.

ACKNOWLEDGMENT

This work was funded by the Member Companies of the Institute of Paper Science and Technology. Their continued support is gratefully acknowledged.

REFERENCES

1. JULIEN SAINT AMAND, F., "Hydrodynamics of Flotation: Experimental Studies and Theoretical Analysis", 1997 TAPPI Recycling Symposium, TAPPI Press, Atlanta, GA, 219-241 (1997).

2. HUNOLD, M., KRAUTHAUF, T., MÜLLER, J., and PUTZ, H.-J., "Effect of Air Volume and Air Bubble Size Distribution on Flotation in Injector Aerated Deinking Cells," *J. Pulp Paper Sci.*, 23(12): J555-J560 (1997).

3. WALMSLEY, M.R.W., "Air Bubble Motion in Wood Pulp Fibre Suspension", APPITA 1992 Proceedings, 509-515 (1992).

4. HEINDEL, T.J., "Bubble Size Measurements in a Fiber Suspension," *J. Pulp Paper Sci.*, 25(3): 104-110 (1999).

5. HEINDEL, T.J., and GARNER, A.E., "The Effect of Fiber Consistency on Bubble Size," *Nord. Pulp Paper Res. J.*, 14(2): 171-178 (1999).

6. HEWITT, G.F., "Flow Regimes", Handbook of Multiphase Systems, G. Hetsroni, Ed., Hemisphere Publishing Corp., New York, Chapter 2.1 (1982).

7. TAPPI, "T 205 om-88 - Forming Handsheets for Physical Tests of Pulp", TAPPI Test Methods 1994-1995, TAPPI Press, Atlanta, GA (1994).

8. TAPPI, "T 413 om-93 - Ash in Wood, Pulp, Paper, and Paperboard: Combustion at 900°C", TAPPI Test Methods 1996-1997, TAPPI Press, Atlanta, GA (1996).

9. HEINDEL, T.J., and MONEFELDT, J.L., "Observations of the Bubble Dynamics in a Pulp Suspension Using Flash X-ray Radiography," *TAPPI J.*, 81(11): 149-158 (1998).

10. CLIFT, R., GRACE, J.R., and WEBER, M.E., "Bubble, Drops, and Particles", Academic Press, New York (1978).

11. ELLENBERGER, J., and KRISHNA, R., "A Unified Approach to the Scale-up of Gas-Solid Fluidized Bed and Gas-Liquid Bubble Column Reactors," *Chem. Eng. Sci.*, 49(24B): 5391-5411 (1994).

12. TSUCHIYA, K., OHSAKI, K., and TAGUCHI, K., "Large and Small Bubble Interaction Patterns in a Bubble Column," *Int. J. Multiphase Flow*, 22(1): 121-132 (1996).

13. DE SWART, J.W.A., VAN VLIET, R.E., and KRISHNA, R., "Size, Structure and Dynamics of 'Large' Bubbles in a Two-Dimensional Slurry Bubble Column," *Chem. Eng. Sci.*, 51(20): 4619-4629 (1996).

14. KRISHNA, R., URSEANU, M.I., VAN BATEN, J.M., and ELLENBERGER, J., "Rise Velocity of a Swarm of Large Gas Bubbles in Liquids," *Chem. Eng. Sci.*, 54: 171-183 (1999).

15. HEINDEL, T.J., and MONEFELDT, J.L., "Flash X-ray Radiography for Visualizing Gas Flows in Opaque Liquid/Fiber Suspensions", 6th International Symposium on Gas-Liquid Two-Phase Flows, Vancouver, BC, ASME Press, New York (June 22-26, 1997).

16. AYYUB, B.M., and McCUEN, R.H., "Probability, Statistics, & Reliability for Engineers", CRC Press, Boca Raton, FL (1997).

Table 1: Experimental conditions.

Fibre Type	Air/water	ONP	CP	NBSK
Average Fibre Length (mm)	0	1.4	2.0	2.8
Ash Content (%)	0	0.6	6.6	0.3
Surface Tension (dynes/cm)	68	53	64	55

Table 2: Summary of bubble data.

Fibre Type	Air/water	ONP	CP	NBSK
Bubble Population	1265	424	219	203
Number of Analyzed X-rays	2	7	5	9
Average Bubble Count per X-ray	632	61	44	23
Average Equivalent Bubble Diameter (mm)	3.0	2.9	4.1	4.2
Standard Deviation (mm)	1.2	2.7	5.5	5.8
Bubble Population with d > 12 mm (%)	0	1.2	2.7	3.9

FIGURE CAPTIONS

Figure 1: Schematic of the experimental set up.

Figure 2: FXR images of the bubble flow conditions in various 1% fibre suspensions for a fixed air injection rate of 2 L/min.

Figure 3: Cumulative number density of the bubble populations.

Figure 4: Cumulative number density of the small bubble ($d \leq 12$ mm) populations.

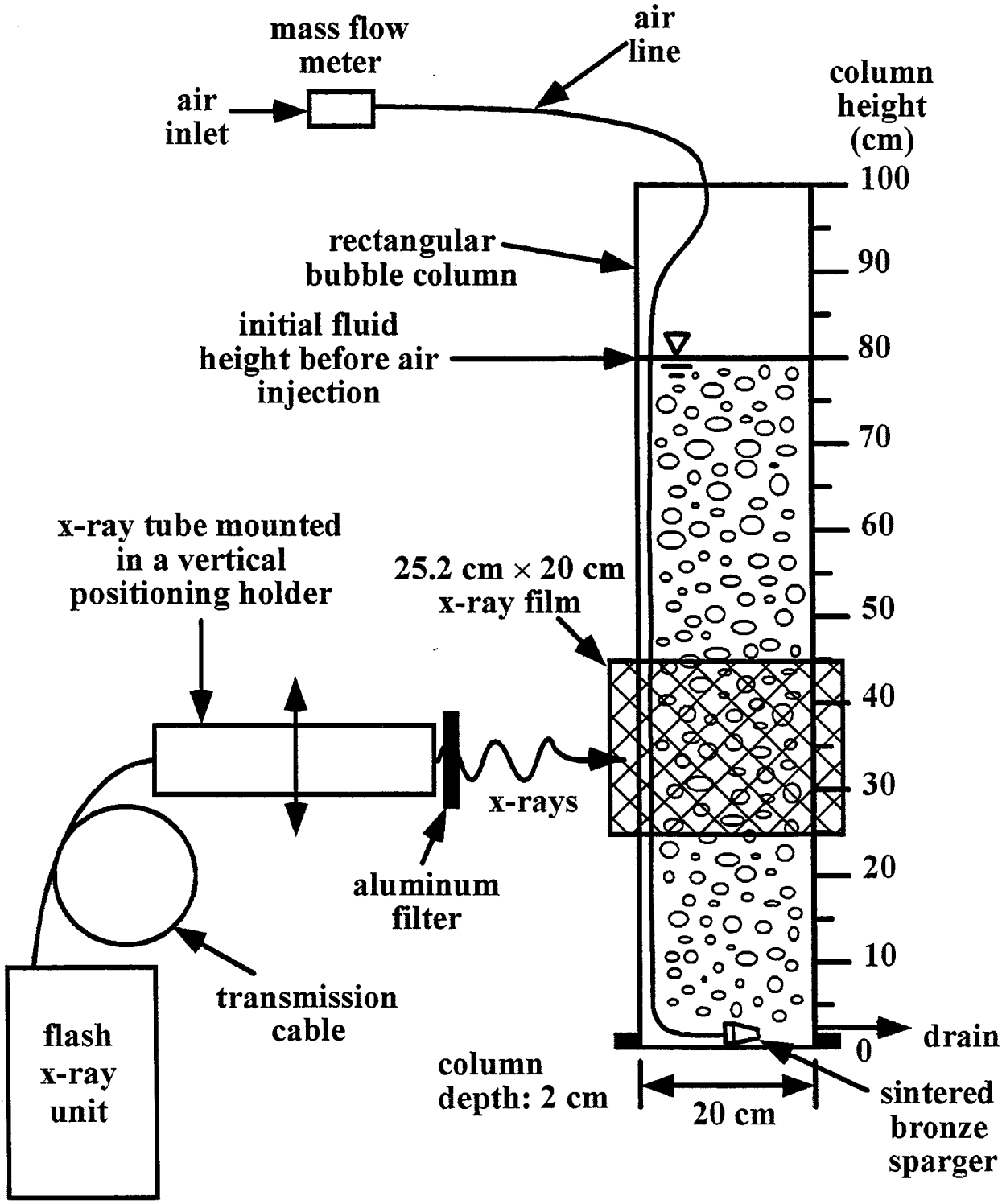
mass flow meter
air line
air inlet
column height (cm)
100
rectangular bubble column
90
initial fluid height before air injection
80
70
x-ray tube mounted in a vertical positioning holder
25.2 cm × 20 cm x-ray film
60
50
40
30
x-rays
aluminum filter
20
10
transmission cable
flash x-ray unit
drain
0
column depth: 2 cm
20 cm
sintered bronze sparger

Figure 1

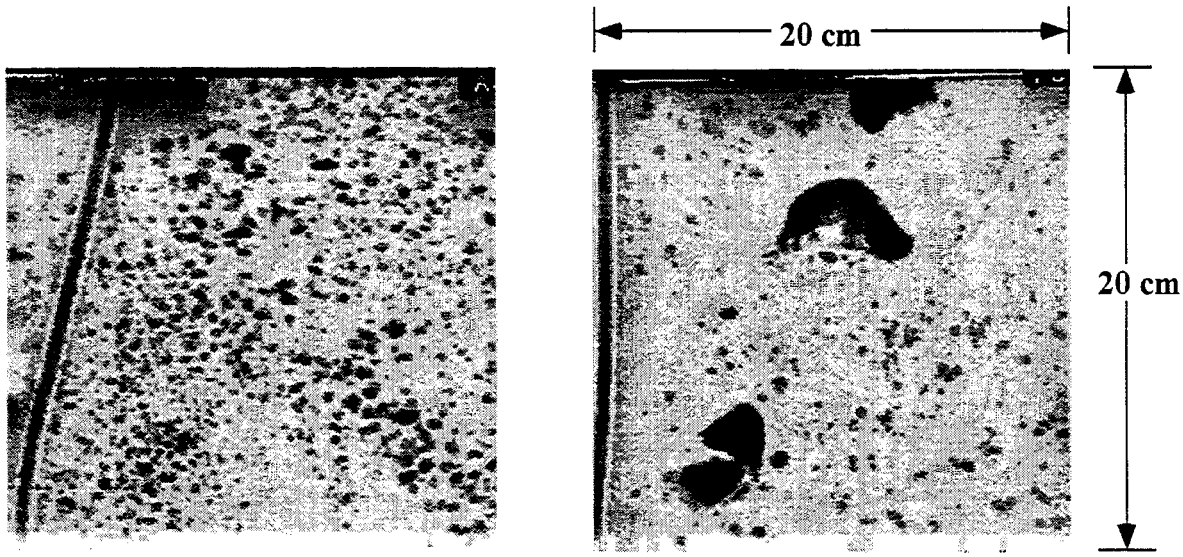

(a) air/water system

(b) 1% ONP

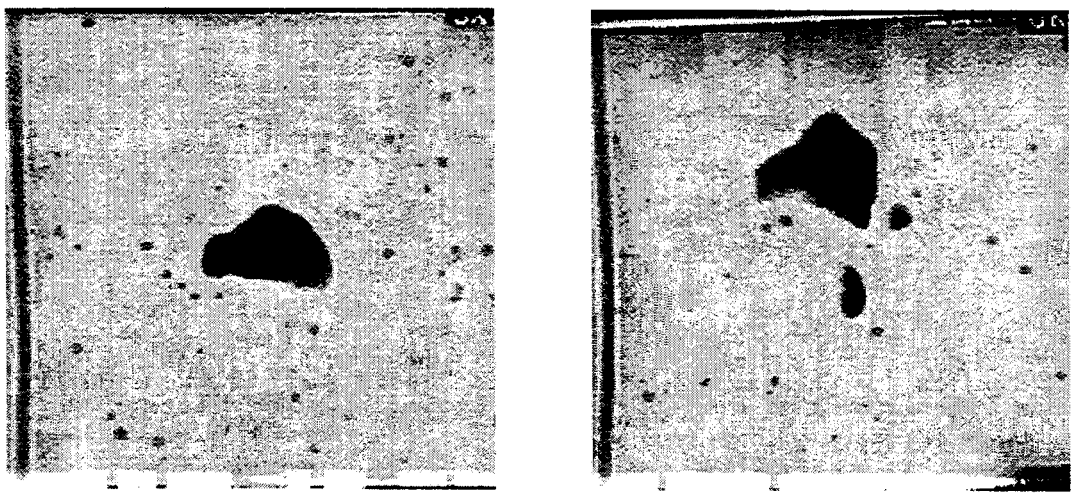

(c) 1% CP

(d) 1% NBSK

Figure 2

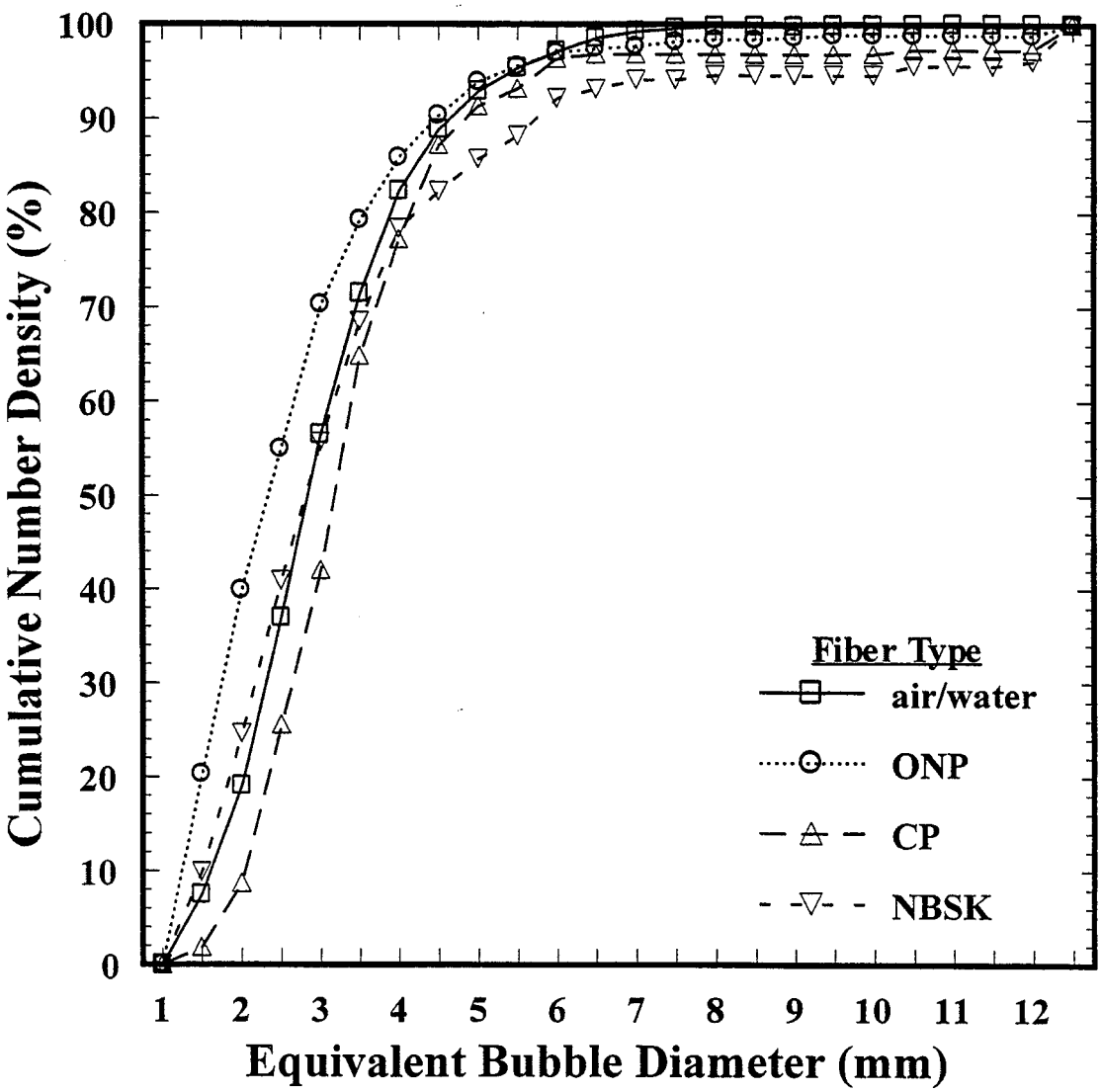
Cumulative Number Density (%)
100
90
80
70
60
50
40
30
20
10
0
1
2
3
4
5
6
7
8
9
10
11
12
Equivalent Bubble Diameter (mm)
Fiber Type
air/water
ONP
CP
NBSK

Figure 3

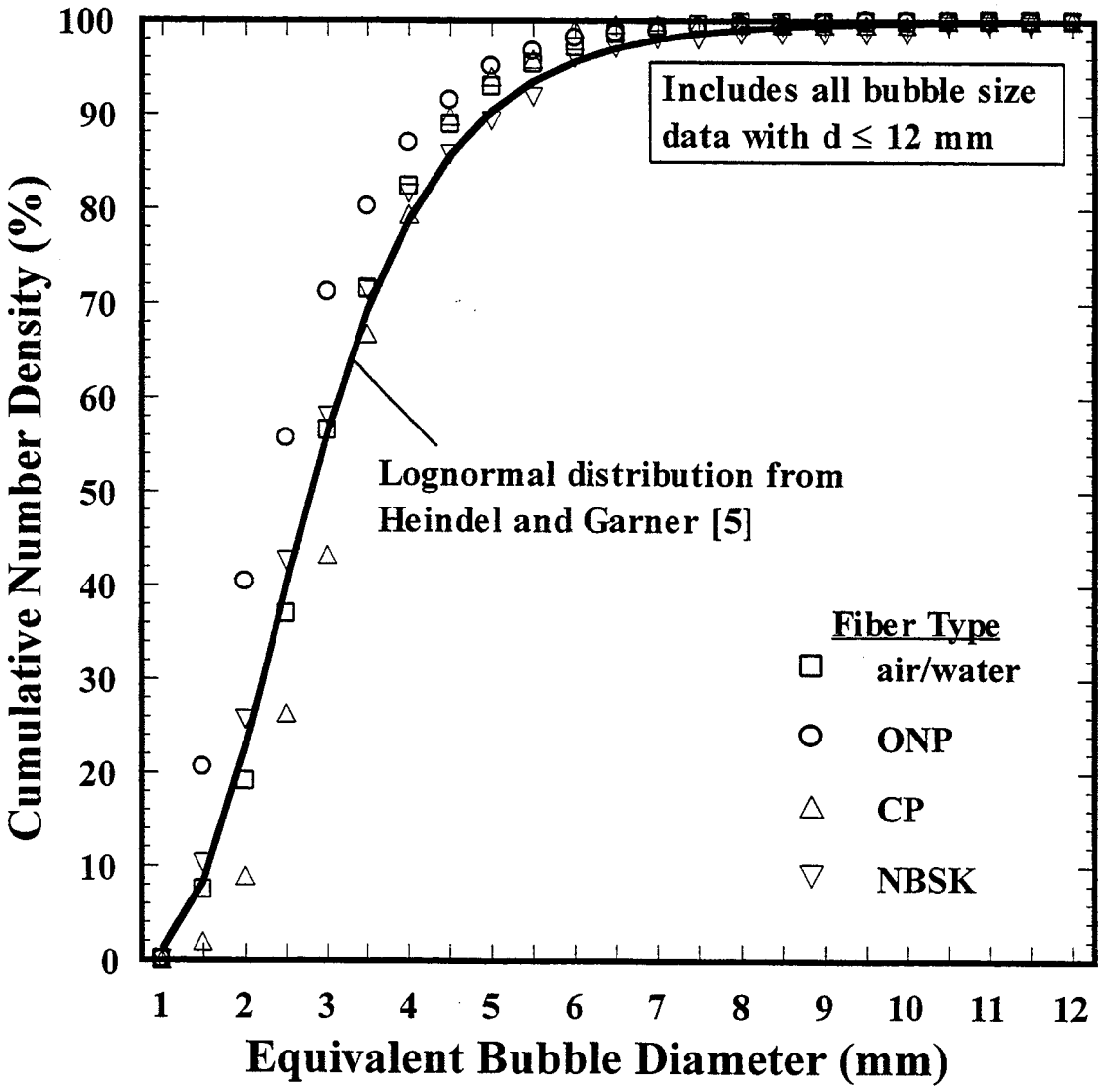
Cumulative Number Density (%)
100
90
80
70
60
50
40
30
20
10
0
1
2
3
4
5
6
7
8
9
10
11
12
Equivalent Bubble Diameter (mm)
Includes all bubble size data with d ≤ 12 mm
Lognormal distribution from Heindel and Garner [5]
Fiber Type
air/water
ONP
CP
NBSK

Figure 4